DURABILITY AND STRENGTH ASSESSMENT OF AAR-AFFECTED BRIDGE DECK PLANKS

Ahmad Shayan[1,*], Riadh Al-Mahaidi[2], Aimin Xu[1]

[1] ARRB Group Ltd, MELBOURNE, Australia

[2] Department of Civil Engineering, Monash University, MELBOURNE, Australia

Abstract

Three prestressed bridge deck planks, removed due to AAR/DEF, were investigated for durability and strength to determine whether similar elements in other bridges need replacement. Compressive strength of cores taken from two planks containing reactive acid igneous rock was 65-70 MPa, whereas that of the plank containing reactive meta-sedimentary rock was 38 MPa (design strength=40 MPa). AAR significantly reduced the elastic modulus of concrete, causing large deflections in planks under loading, giving adequate warning before failure at ultimate load capacity.

Ultimate strength was not significantly affected by the AAR, indicating that performance of planks was governed by prestressing wires and their bond strength, which was not significantly affected by AAR at present age. Residual expansion potential of concrete was high; indicating further deterioration can be expected. Despite adequate ultimate strength at present, long-term performance of planks is at risk due to the large residual expansion potential.

KEYWORDS: prestressed elements, AAR, DEF, strength, load-capacity

1 INTRODUCTION

The Bridge investigated was built in 1989 and consisted of six spans, with 16 precast, prestressed deck planks per span, supported on piers, comprising two cast-is-situ columns and crosshead. Figure 1 shows a general view of the bridge and some of the removed planks. Figure 2 shows parallel longitudinal cracking on plank soffits, and reinforcement details in the cross section of planks. Shayan & Morris [1] attributed the cracking to alkali-aggregate reaction (AAR).

Original drawings of the planks specified minimum 28-day compressive strength of 40 MPa, and transfer strength of 35 MPa. The calculated hog was 40 mm at 28 days, based on the assumptions of density = 2600 kg/m^3; elastic module at transfer = 36.7 GPa; steam curing at 70°C for 8 hours (anecdotes indicate temperatures well above 70°C); plank's own weight = 6.5 tons; storage after steam curing in open air at 20°C average temperature, and RH of 50-75%.

Earlier investigation [1] indicated compressive strength and elastic modulus had decreased by as much as 30% and 50%, respectively. The extensive AAR and significant strength reductions of the pre-stressed planks were of concern as excessive expansion could cause loss of prestress and bond failure, resulting in sudden collapse under load.

In 2003 the bridge deck was removed and the affected planks stored on-site. As there are many similar bridges in the region, with the same problem, assessment of the mechanical properties and load capacity of the discarded planks became essential for making sound decisions on the rehabilitation strategy of these bridges. This paper details durability assessment and full scale strength testing of some discarded planks, to clarify whether the load capacity of cracked piles is adequate under service conditions, or they need to be replaced.

2 EXPERIMENTAL WORK

Three planks of varying degrees of cracking were selected for investigation, based on the visible extent of cracking (Table 1). Due to the difficulty of handling the 11.8 m long (6.5-ton) planks, each was cut on site into two segments of equal length for ease of transportation. One segment from each visual class was allocated for durability assessment and the other segments for strength assessment. One of the two segments from the worst damaged plank was used for both purposes. The origin of the general purpose (GP) cement used in the planks is unknown.

* Corresponding author : ahmad.shayan@arrb.com.au

2.1 Determination of durability properties of the concrete

Eleven cores (95 mm Ø) were taken from each half-plank, across the full thickness of the whole plank (380 mm) for petrographic examination, scanning electron microscopy (SEM) and energy-dispersive X-ray (EDX) analysis, determination of cement content (acid digestion), residual water-soluble alkali content of concrete, compressive strength, splitting tensile strength, residual expansion (38°C, 100% RH), and maximum expansion potential (38°C, 1M NaOH).

In addition, the coarse aggregate was separated from two planks containing two different aggregates (planks M12 and M67) by crushing about 50 kg portions of each and hand picking the coarse aggregate. They were then tested by the Australian AMBT (RTA T363, similar to ASTM C1260) and CPT (RTA T364, similar to ASTM C1293) to assess their residual reactivity.

Representative segments of planks were cut (600×380×300 mm) and fitted with Demec length measurement studs, and then moved to accelerated conditions at 38°C, 100% RH for expansion measurement. Moreover, square grids of 3x3 measuring points were installed on the surface of the planks (soffit), by drilling holes at 200mm centres and gluing in 15 mm long stainless steel screws (flush with the surface) suitable for locating the Demec Gauge measuring arms. The grid allowed measurement of expansion in both longitudinal and transverse directions. A moisture- and alkali-resistant epoxy resin was used for fixing the studs and screws. Figure 3 represents the grids for both blocks and planks.

2.2 Strength assessment of planks

Testing and theoretical analysis was conducted on four half-planks (5.8 m long) to determine their load rating, as well as ultimate strength, ductility and deflection. Figure 4 shows four-point loading of a simply supported plank, using a computer controlled 1000 kN capacity jack and data acquisition system. The arrangement approximates the loading from a dual axle. The instrumentation included load cells and strain gauges on both the prestressing strands and concrete. The tests used load control at a quasi-static rate of loading, typically 20 kN/minute. They were first loaded and unloaded three times to half their expected ultimate capacity, after which they were loaded to failure. Loading was halted several times during the testing to visually record the extent of cracking at each load level.

During testing the total load in the jack was measured by a load cell. The reactions at each support end were measured by four load cells placed in pairs. The testing for each plank included measurements of:

- Strain in three prestressing wires, at two locations along the length of the plank, and in one prestressing wire at a location 1m from the support
- Strain in the concrete at two locations on the top surface at mid-span locations
- Deflection at five locations along the length of the plank soffit, including both reaction ends. The purpose of the latter was to account for support settlement since elastomeric pads were used between the plank soffit and the reaction bars
- Measurement of initial stress in prestressing wires, due to pre-tensioning. This was measured after the completion of loading tests by progressive removal of the surrounding concrete from the bond zone of a targeted prestressing wire, working from the end and progressively removing the concrete along one metre length of the wire, and recording strain changes at one metre from the end.
- Tensile strength testing of prestressing wires, taken from minimal stress areas, and determination of elastic modulus on drilled cores.
- Nonlinear finite element analysis (to be reported elsewhere [2]).

3 RESULTS AND DISCUSSION ON DURABILITY ASSESSMENT

3.1 Visual observations

Parallel longitudinal cracking was present in all planks. The AAR rimming of aggregate pieces, revealed on the fracture surfaces of drilled cores (Figure 5), was weak in Plank M12, strong in M67 (fissile aggregate), and moderate to strong in M26. Much more aggregate internal cracking was seen in M67 than M12; M26 being intermediate. The difference between the visual appearance of the reacted aggregate particles in M67 and the other two planks, is probably related to its fissile nature, compared to the denser nature of the acid igneous rock used in M12 and M26.

To quantify the visual observations, AAR-related features of cores, earlier identified in the planks [1], were counted on two or three cores from each plank (on three lines drawn at 120 degrees on each core) and added up for individual planks, and then converted to a percentage of the total number of aggregate pieces intersected by the lines. These features included internally cracked aggregates, reaction rims, gel-filled voids, etc. This gave the percentage of reacted aggregate pieces in the planks, being 7%, 70% and 31% for planks M12, M67 and M26, respectively.

3.2 Petrographic description of concrete

Planks M12 and M26 had the same coarse aggregate, being a porphyritic acid igneous rock (dacite-rhyodacite) comprising very fine quartz/feldspar matrix embedding phenocrysts of feldspar and embayed quartz, as well as mica and pyroxene. The sand contained moderately to highly strained quartz. Both aggregates are considered to be prone to AAR.

The coarse aggregate in M67 was a greywacke/hornfels, comprising a fine matrix of quartz and mica surrounding coarser quartz and feldspar. The micaceous matrix showed preferred orientation, promoting a fissile nature. Coarser quartz crystallites showed sutured grain boundaries and moderate to high strain. Both the coarse and fine aggregates are considered reactive in high alkali concrete.

The cementitious matrix in M12 exhibited microcracking, and contained air voids thinly lined with ettringite. AAR gel was seen around some aggregate pieces and filling some cracks. These features were much stronger in M67. Significant parallel, branching microcracking was present in M26. The petrographic analysis showed AAR signs in all the planks. Considerable carbonation was noted along the length of these cracks, indicating that they were old cracks.

3.3 SEM /EDX analysis

Around 200 SEM/EDX analyses were made on microstructural features and chemical composition of secondary reaction products found in concrete specimens. All the planks contained typical AAR products (Figure 6) in the form of AAR gel and crystalline products. The cement paste in the planks was often enriched in alkali and Si, and appeared to be impregnated with AAR gel. In some locations in the paste (plank M12) Na-rich crystals, probably NaOH were seen (Figure 6), and in other locations fibrous crystals of sodium carbonate had formed (plank M67); the latter as a result of exposure to air. AAR products were far more abundant in plank M67 than plank M12. The extents of AAR was similarly large in Plank M26, despite the fewer aggregate particles that exhibited AAR rimming

In addition to AAR products thin layers of ettringite were noted in plank M12, at the cement-aggregate interfacial zones, which indicated mild DEF. However, extensive formation of ettringite mats was noted in planks M67 (eg. Figure 7) and M26, which indicate much stronger cases of DEF. Planks M67 and M26 may have been subjected to a significantly higher curing temperature than M12. In all planks, ettringite was usually formed close to the AAR gel (eg. Figure 8), which is a common observation in many similar Australian cases (Shayan [3]). It is likely that the extent of damage to the planks is related to the effect of high curing temperature (magnitude and duration) on AAR and DEF, both of which are exacerbated at high temperature.

In the more extensively damaged planks, cracks filled with AAR gel at the boundaries of aggregate particles shown in Figure 5 and other similar samples, were around 200 μm in width. Compared to the aggregate size of 20 mm, this represents a free expansion of 1% or 10,000 μstrain. Occasional crack filled with AAR gel (Figure 6) measured as wide as around one millimetre (i.e. 5% expansion). Although the longitudinal expansion of the planks is suppressed by the prestressing wires, expansion must have occurred in the transverse direction, which caused the observed cracking. The restrained AAR expansion increases the prestress in the wires, which could increase the flexural capacity of planks.

3.4 Cement content, residual alkali content and VPV

Cement content, determined by acid digestion, and water-soluble alkali content of concrete, determined on representative pulverised core samples are given in Table 2. The cement contents are high, which is common for precast, prestressed structural elements. Part of the differences among the planks could be related to sampling variation and the amount of aggregate component present in the sample. It could probably be said that the cement content of the planks was around 500 kg/m^3. The residual alkali contents of the planks were also high (~ 3 kg/m^3), considering that significant reaction has already occurred in the planks. This indicates that the planks would still have considerable residual expansion capacity.

The volume of permeable voids (VPV) results, determined in accordance with ASTM C642 on the crack-free, middle portions of a core from each plank (four 50 mm thick segments), are given in Table 2. The VPV is important in relation to transport mechanisms inside the concrete. In Australia, Vic Roads specification section 610, clause 610.06, requires the VPV of test cores at the age of 28 days not to exceed 14% for the highest strength grade listed (55 MPa). The VPV values for planks do not follow their visual damage ranking. This probably arose because VPV was measured on core slices from the centre of planks, which did not reflect their external cracking.

3.5 Compressive and tensile strength

Table 2 gives the average and range of compressive strength determined on three cores, and average of splitting tensile strength on two cores (95 mm Ø x 190 mm long, and shows that plank M12 had the highest strength, followed by Planks M26 and M67, whereas plank M26 was visually more damaged. Plank M67 contained the sedimentary, fissile aggregate which exhibited the strongest rimming. It seems that in addition to the extent of AAR, the type of aggregate could have affected the compressive strength.

The core strength values given in Table 2 exaggerate the strength of the planks, as the soundest parts of the cores were tested. Cores from plank M26 showed a wide strength range, probably reflecting variable microcracking. Swamy [4] reported that AAR expansion in experimental beams and columns resulted in very large concrete and steel strains and caused significant reductions in their engineering properties. Nevertheless, the strength values for planks M12 and M26 are higher than the specified values, but not for Plank M67.

The splitting tensile strength of cores did not follow the trend of visual damage or compressive strength, and Plank M26 and M12 had the same strength values. The results disagree with other reports [5], which stated that this test was a better predictor of AAR damage than compressive strength. The disagreement could have arisen from variation in crack orientation in relation to the loading direction for the specific specimens, and the conclusions of that report [5] could still generally be valid.

3.6 Residual reactivity of coarse aggregate separated from planks

The results of AMBT and CPT conducted on the coarse aggregates recovered from planks are given in Figure 9. They indicate that the residual reactivity of the aggregates is still high, i.e., they still contain reactive components that could further react in the planks. Given the sufficient amounts of residual alkali in the planks, they are expected to continue to expand in the future.

3.7 Residual expansion of concrete measured on cores

Expansion results largely relate to planks M12 and M67, as plank M26 was load-tested much later and was not available at the same time as them. Figure 10 show the significant, unrestrained residual expansion for cores from planks M12 and M67, stored at 38°C, 100% RH and in 1M NaOH at 38°C. The residual expansion was larger for M12 than M67, which is attributed to the more extensive reaction exhibited by M67 to-date; leaving less potential for further reaction. This potential is suppressed by the prestressing wires and reinforcement bars in the planks, and only a proportion of it would eventuate in the future. Tomita et al. [6] stated that 50% of core expansion would eventuate in the field, whereas Blight and Ballim [7] found consistency between the two. In fact, the type of element studied may influence the outcome.

Comparison between the two storage conditions shows that the expansion in 1M NaOH solution is continuing at a higher rate compared to that achieved at 38°C, 100% RH. This arose because of the new supply of alkali, and indicates the residual reactivity potential of the aggregate, as verified above. The magnitude of residual expansion of cores was similar to those measured by the CPT method on the recovered coarse aggregate at same age, indicating that both measure free expansion potential.

3.8 Residual expansion of blocks cut from the planks (38°C and 100% RH)

Figure 11 shows the results of expansion measurements made on several locations on each block surface, as illustrated in Figure 3. The expansion curves in Figure 11 indicate that longitudinal expansion is rather low, being an average of around 0.03%. However, expansion in the transverse direction ranged from 0.08% to 0.30% for plank M12 and 0.044% to 0.15 % for plank M67, respectively. These expansion values are far smaller than the free expansion of 1% estimated earlier from the width of gel-filled cracks. They are also smaller than the free expansion measured on cores and by the CPT method. Nevertheless, they are considered deleterious, and would be expected to lead to further cracking or crack widening in the future.

3.9 Residual expansion of planks exposed to outdoor exposure conditions

Figure 12 shows the results obtained for planks M 12 and M 67. As expected the planks did not expand in the longitudinal direction. There was even minor shrinkage due to surface drying of the concrete in the period of measurement. However, relatively large expansions occurred in the transverse direction. The transverse expansion values measured on the different points on plank M 12 ranged from 0.030% to 0.090% in the 8-months period. The corresponding values for plank M 67 were 0.032% to 0.065%. Again, it is seen that plank M 12 exhibited a larger expansion potential due to the lower extent of AAR already observed for this plank.

The core expansion values are much larger than the corresponding values mentioned above, which indicates that not all the unrestrained core expansion would occur in the whole element, in agreement with [6].

Nevertheless, these values indicate that further deterioration would take place in the planks in the form of new cracking or widening of existing cracks. Therefore, it is likely that the bond strength of the prestressing wires could adversely be affected with time, which may compromise the integrity and safety of the prestressed planks.

4 RESULTS AND DISCUSSION ON STRENGTH ASSESSMENT

4.1 Strength properties of component materials in tested planks

Table 3 shows the concrete strength and elastic modulus results for the four load-tested planks. The strength results are similar to those the companion planks (Table 2), allocated to durability tests. Again, plank M67 showed the lowest strength, and the elastic modulus was correspondingly very low (vs. elastic modulus of 36.7 GPa, required at transfer of prestress). Based on previous studies [8], the load capacity of planks would also be expected to follow this trend, but this was not the case (see below).

Table 4 shows the tensile strength results for the prestressing wires, indicating an average ultimate tensile strength of 1979 MPa. The average modulus of elasticity of the wires was 208 GPa. These values were used in the NLFEA, reported elsewhere [2].

4.2 Results from plank tests

The ultimate loads and corresponding moment capacities are summarised in Table 5. The moment-deflection plots for the units are given in Figure 13. Unlike the core strength results, the four planks exhibited very similar behaviour, as is evident from the moment-deflection plots. These plots include the first stage of cyclic loading. After the first cycle of loading, no significant change was observed on reloading. When 300 kN was reached in the cyclic loading stage, only minor flexural cracks were observed. The lower initial slope of the curve of plank M67 (B2) is indicative of the lower modulus of elasticity of its concrete, as noted in Table 3. During the testing of plank M26 (B4), loud noises were heard in two instances post 300 kN load, possibly indicating bond failure between the concrete and some of the strands. This could be the reason that this plank gave the lowest load capacity.

Failure of all of the planks occurred when the compression concrete at mid-span crushed. At failure, the prestressing wires were close to or beyond the proof (yield) strain. Cracking was observed at a jack load of approximately 300 kN for all planks. At failure, cracking had developed throughout the constant moment region, and significant diagonal tension (shear) cracking developed outside the constant moment region (Photo in Figure 13).

The measured strains in the prestressing wires at mid-span are plotted in Figure 13. They exclude the initial pre-tensioning strain in the wires. The stress in the wire was 208 GPa, as calculated from its measured elastic modulus. The wire was in a region that had not been affected by the ultimate load test, and was subjected only to prestress loads (no other loads). The average stress in the prestressing wire was 990 MPa. By adding the initial prestressing strains to the measured strains near failure, it became evident that the prestressing wires at mid-span had yielded near the failure time of the planks.

Concrete strains at mid-span are also plotted in Figure 13. They show that the planks exhibited similar behaviours, regardless of the degree of AAR. These results agree with earlier studies [eg. 9-12] which found no significant AAR effect on the failure behaviour of prestressed or reinforced beams. Despite compressive strength reductions of 40-50% in AAR-affected concrete, the ultimate load capacity was reduced by only 1-20% [13]; the effect being smaller for larger elements.

This is due to prestressing effects brought about by AAR expansion in reinforced elements. Swelling pressures as high as 4 MPa have been measured in AAR-affected concrete [12]. AAR expansion of 0.08-0.14% has been reported to cause a prestress of 3.3 MPa in reinforced specimens

[14]. The prestressing effect of AAR on the reinforced elements appears to enable them to retain their shear strength, whereas the AAR microcracking reduces the tensile strength and elastic modulus of concrete. For this reason, full-scale testing to design load was said [12] to better evaluate the safety and integrity of the structural elements, compared to testing cores.

Although the literature states that AAR has little overall effect on the performance of reinforced concrete structure, it must be noted that this may not apply to all elements. For example, smaller reinforced columns were more seriously affected than larger ones [13].

5 CONCLUSIONS

All the planks exhibited distinct signs of AAR and some DEF. The planks exhibited large residual expansion potentials due to sufficient amounts of reactive components and alkali being present to cause further expansion and cracking. The ultimate strength of the planks was not significantly affected by the AAR damage, which appeared to have a stronger influence on the deflection of the planks, due to the significant reduction of elastic modulus of the AAR affected concrete. These findings agree with the published literature. In addition, prior to failure the planks exhibited significant cracking over the central constant moment area. Adequate warning of pending failure was provided through substantial deflections as the applied load approached the ultimate failure value; well after yield stress was reached in the prestressing wires. Although the planks performed satisfactorily under loading, their long term durability and safety is at risk due to their high residual expansion property. Therefore, the long term performance and safety of these planks cannot be guaranteed.

6 ACKNOWLEDGEMENTS

The authors are grateful for financial support from RTA, NSW; Main Roads QLD; VicRoads; DIER Tasmania; Transport SA; DI&P, NT and Roads ACT. The opinions expressed in this paper are those of the authors and not necessarily reflect the policies or practices of the supporting organisations.

7 REFERENCES

[1] Shayan, A, and Morris, H (2002): Cracking in precast, prestressed deck planks in two bridges and rehabilitation options. ACI Materials Journal (99): 165- 172.

[2] Al-Mahaidi, R, Shayan, A, and Gamage, K (2008): Strength assessment of prestressed concrete bridge deck planks damaged by AAR. Proceedings of the 23rd ARRB Conference, Adelaide, Australia, 30 July- 1 August 2008: accepted for publication.

[3] Shayan, A (2003): AAR in Australia and recent developments. International Seminar on Road Construction Materials, Kanazawa University, Japan, 28 October - 01 November: invited keynote lecture.

[4] Swamy, RN (1995): Effects of alkali-aggregate reactivity on material stability and structural integrity. Proceedings of the CANMET/ACI International Workshop on AAR, Dartmouth, Nova Scotia, 1-4 October: 293-309.

[5] Bremner, TW, Boyd, AJ, Holm, TA, and Boyd, SR (1995): Tensile testing to evaluate the effect of AAR in concrete. Proceedings of the CANMET/ACI International Workshop on AAR, Dartmouth, Nova Scotia, 1-4 October: 311-325.

[6] Tomita, M, Miyagawa, T, Nakano, K (1989): Basic study for diagnosis of concrete affected by ASR using drilled concrete cores. In: Okada, K, Nishibayashi, S, and Kawamura, M (editors): Proceedings of the 8th International Conference on Alkali-aggregate Reaction in Concrete, Kyoto: 779-784.

[7] Blight, GE, and Ballim, Y (2000): Properties of AAR-affected concrete studied over 20 years. In: Bérubé, MA, Fournier, B, and Durand, B (editors): Proceedings of the 11th International Conference on Alkali-Aggregate Reaction in Concrete, Québec, Canada: 1109-1118.

[8] Alexander, MG, Blight, GE and Lampacher, BJ (1992): Pre-demolition tests on structural concrete damaged by AAR. In: Poole, AB (editor): Proceedings of the 9th International Conference on Alkali-Aggregate Reaction in Concrete, London, United Kingdom: 1-8.

[9] Abe, M, Kikuta, S, Masuda, Y and Tomozawa, F (1989): Experimental study on mechanical behaviour of reinforced concrete members affected by alkali-aggregate reaction. In: Okada, K, Nishibayashi, S, and Kawamura, M (editors): Proceedings of the 8th International Conference on Alkali-aggregate Reaction in Concrete, Kyoto: 691-696.

[10] Koyanagi, W, Rokugo, K and Ishida, H (1986): Failure behaviour of reinforced concrete beams deteriorated by alkali-silica reaction. In: Grattan-Bellew, PE (editor): Proceedings of the 7th

International Conference on Alkali-Aggregate Reaction in Concrete, Ottawa, Canada: 141-145.
[11] Fujii, M, Kobayahi, K, Kojima, T and Maehara, H (1986). The static and dynamic behaviour of reinforced concrete beams with cracking due to alkali-silica reaction. In: Grattan-Bellew, PE (editor): Proceedings of the 7th International Conference on Alkali-Aggregate Reaction in Concrete, Ottawa, Canada: 126-130.
[12] Blight, GE (1996): Engineering properties of reinforced concrete damaged by AAR. In: Shayan, A (editor): Proceedings of the 10th International Conference on Alkali-aggregate Reaction in Concrete, Melbourne, Australia: 987-994.
[13] Takemura, K, Ichitsubo, M, Tazawa, E and Yonekura, A. (1996): Mechanical performance of ASR affected nearly full-scale reinforced concrete column. In: Shayan, A (editor): Proceedings of the 10th International Conference on Alkali-aggregate Reaction in Concrete, Melbourne, Australia: 410-417.
[14] Smaoui, N, Bérubé, MA, Fournier, B, and Bissonnette, B (2004). Stresses induced by ASR in reinforced concrete incorporating various aggregates. In: Tang, M, and Deng, M (editors): Proceedings of the 12th International Conference on Alkali-Aggregate Reactions in Concrete, Beijing, China: 1191-1201.

Table 1: List of all the six half-planks and testing conducted

Plank ID	Laboratory designation	Visual damage class	Half-Plank ID	Test schedule
M12	C07/ 1532	Least	M12	Durability
			M12 (B1)	Strength assessment
M67	C07/ 1533	intermediate	M67	Durability
			M67 (B2)	Strength assessment
M26	C07/ 1664	Worst	M26 (B3)	Strength assessment
			M26 (B4)	Durability & Strength

Table 2: Concrete properties determined on core samples taken from planks

Plank ID	Cement content (kg/m3)	Na_2Oeq†	Compressive strength (MPa)	Splitting Tensile Strength (MPa)	VPV‡ (%)
M12	475	2.61	76.7 ± 2.7	5.3	12.6
M67	533	3.38	39.2 ± 8.6	5.4	12.8
M26- surface	-	3.41	60.3 ± 10	4.9	15.4
M26- interior	563	3.00			
† $Na_2Oeq = Na_2O + 0.658\ K_2O$; dry mass basis ‡ Volume of permeable voids					

Table 3: Compressive strength and elastic moduli of cores taken from planks

Plank no.	M12 (B1)	M67(B2)	M26 (B3)	M26 (B4)
Compressive strength (MPa)	69.6 70.4	36.5 40.0	68.7 66.1	72.2 67.0
Average	70.0	38.3	67.4	69.6
Elastic modulus (GPa)	28.68 28.20	14.90 15.93	26.57 26.02	27.61 26.11
Average	28.44	15.41	26.30	26.86

Table 4: Test results for prestressing wires (in MPa)

	0.2% proof stress, fp_y	Ultimate tensile strength, fp
Sample 1	1831	1970
Sample 2	1842	1988
Sample 3	1852	-
Average	1841	1979

Table 5: Ultimate loads and moments from testing

Plank no.	Experimental ultimate load 2Pu (in kN)	Experimental moment capacity Mu (in kN·m)
M 12 (B1)	614	691
M 67 (B2)	591	665
M 26 (B3)	585	658
M 26 (B4)	557	627

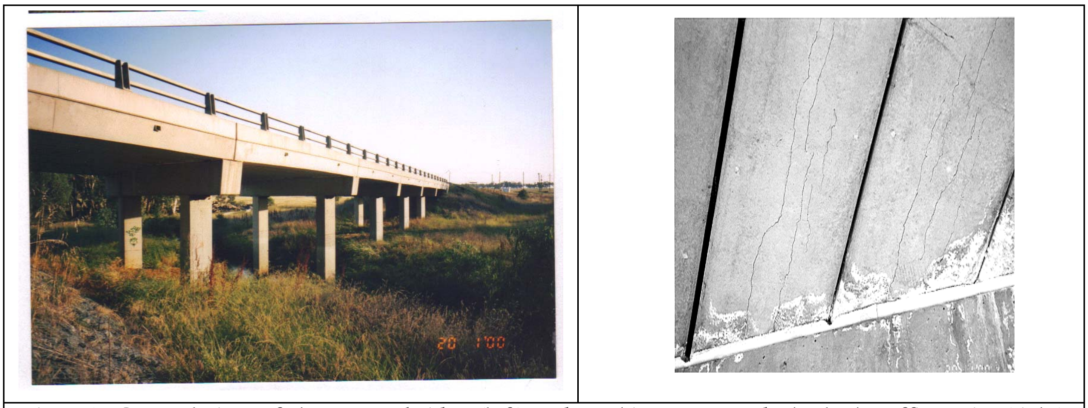

Figure1- General view of the 7-span bridge (left) and cracking seen on deck plank soffit onsite (right)

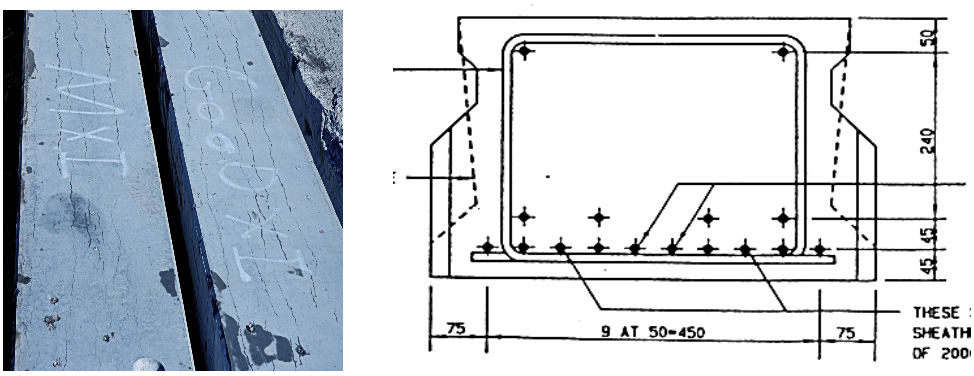

Figure 2: cracking in planks M67 and M12 (left), and cross section of planks (right)

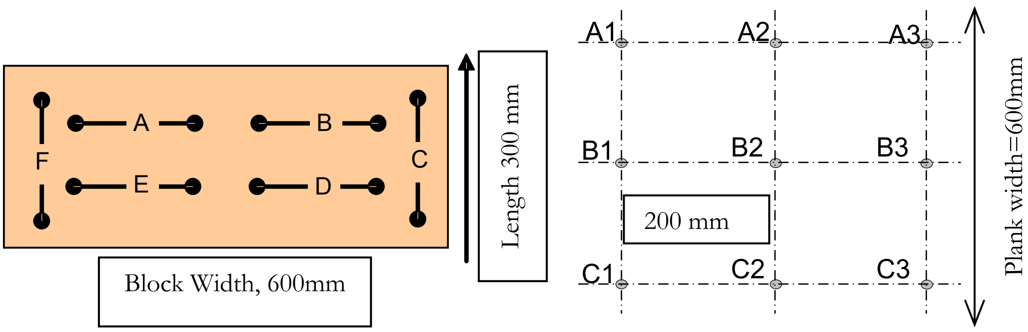

Figure 3: Grids for expansion measurement on surfaces of Blocks (left) and whole Plank (right). Note different directions for planks and blocks

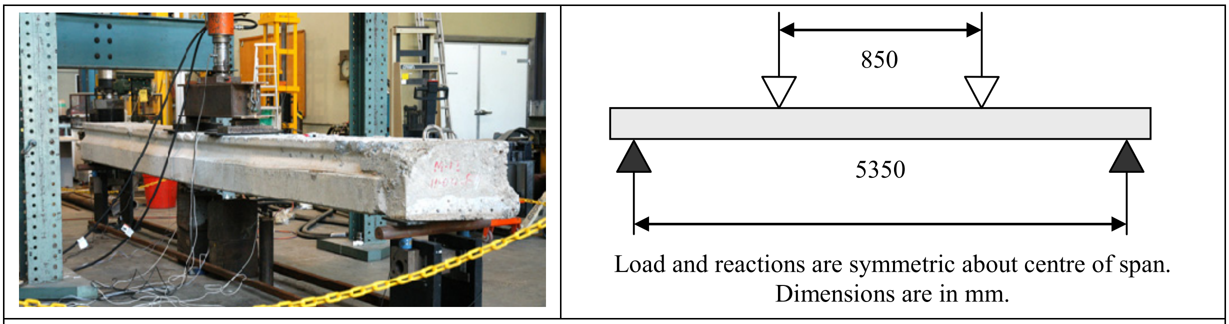

Figure 4: Representative loading arrangement for the planks

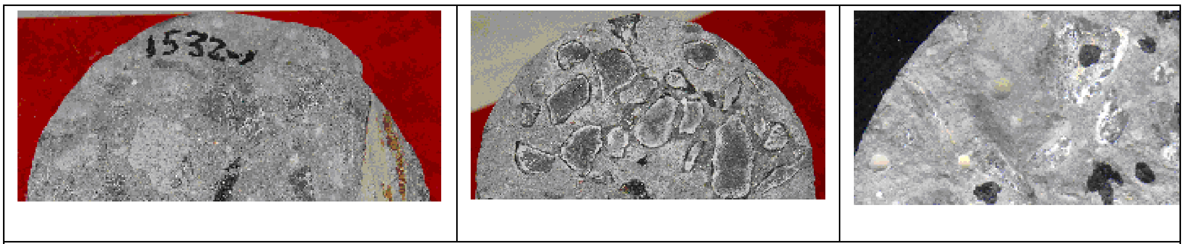

Figure 5: Representative views of fracture surface of cores from M12 (left), M67 (middle), and M26 (right), showing reaction rims on aggregate particles.

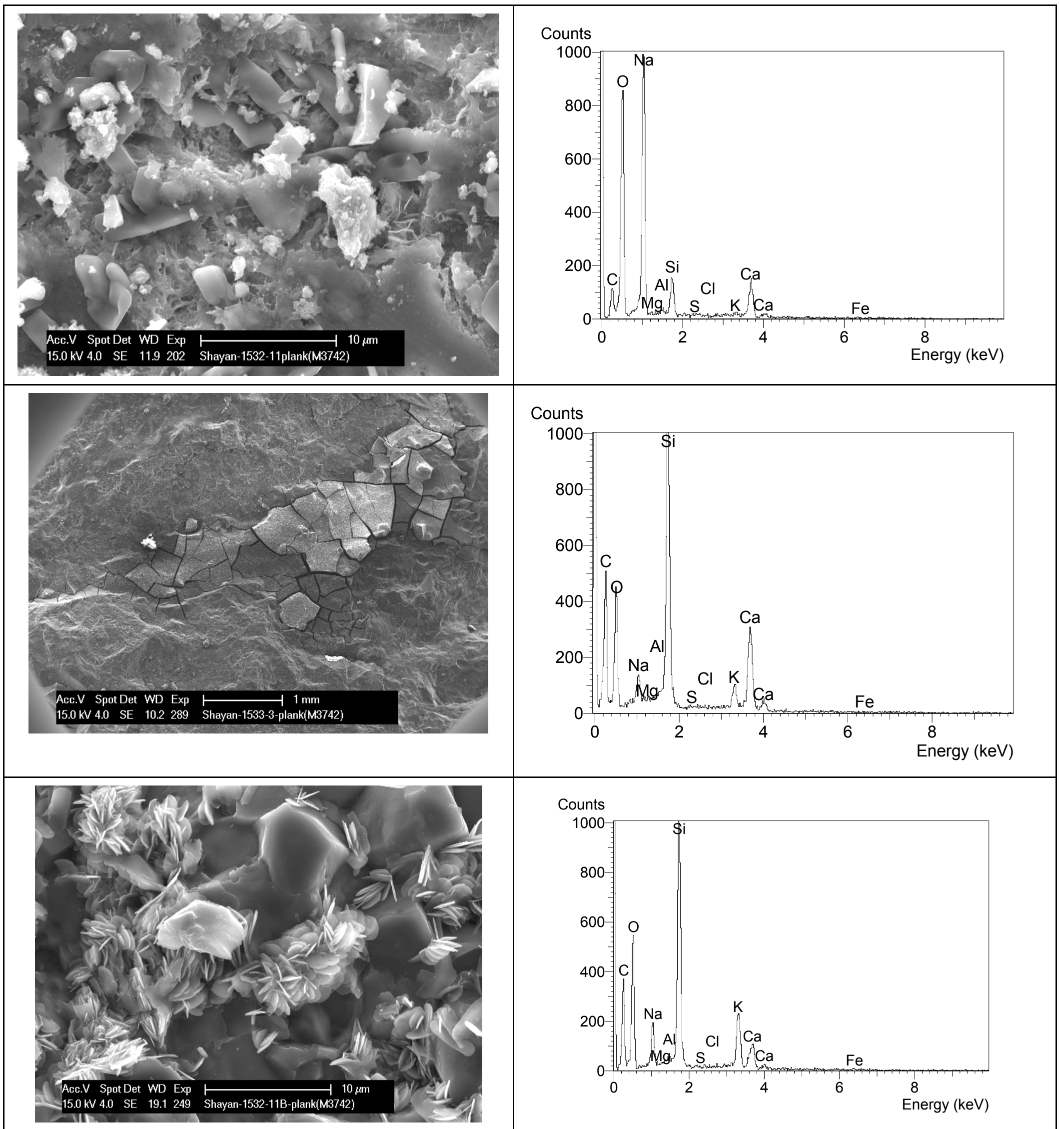

Figure 6: SEM observations showing crystalline Na-hydroxide in paste (top), AAR gel in crack (middle) and AAR rosettes formed inside the aggregate particle. This is common to all planks

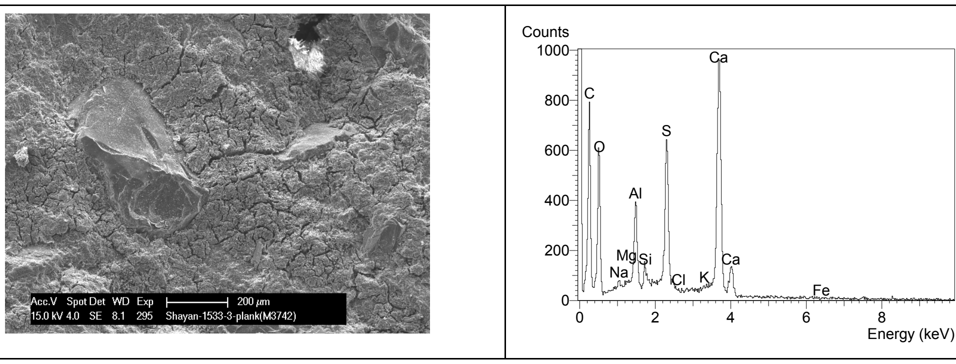

Figure 7: SEM view of ettringite mat formation at aggregate-paste interface, indicative of DEF

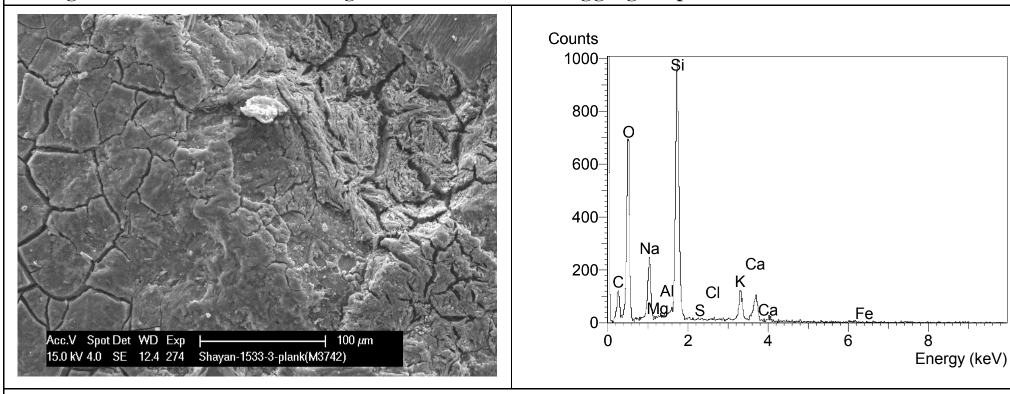

Figure 8: SEM image showing association of AAR (left) and DEF (right) in plank M67. The EDX spectrum is for the AAR gel. The ettringite EDX was identical to that shown in Figure 7.

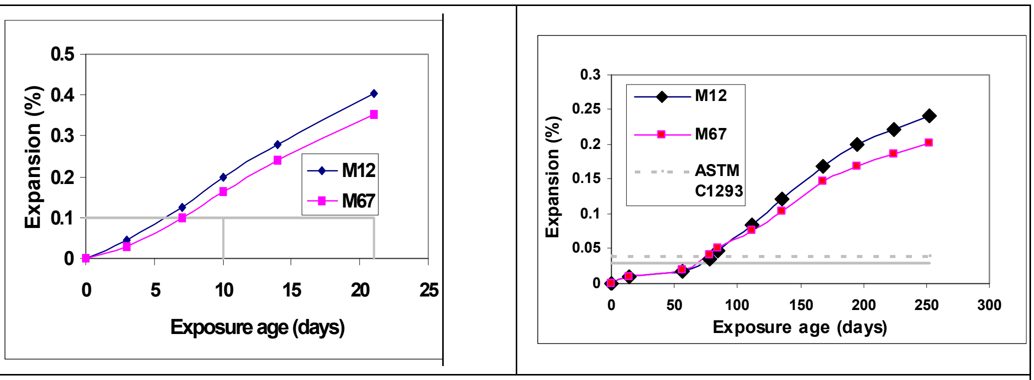

Figure 9: AMBT (left) and CPT (right) expansion curves for the two corse aggregates indicated.

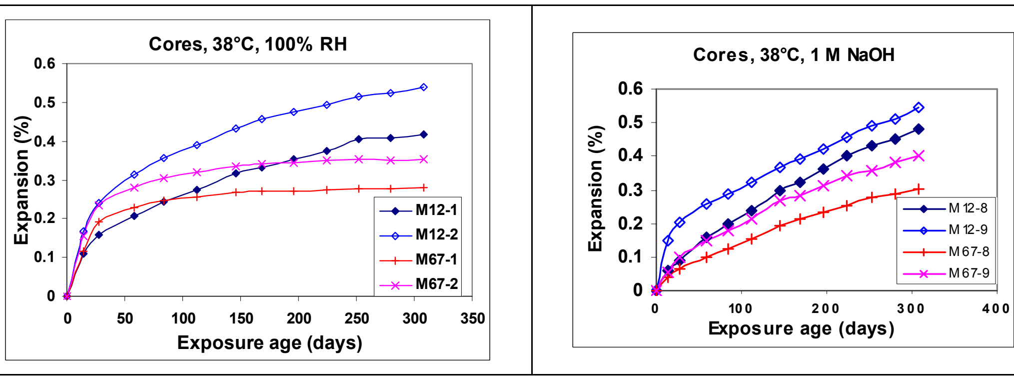

Figure 10: Expansion curves for cores stored under the different conditions indicated

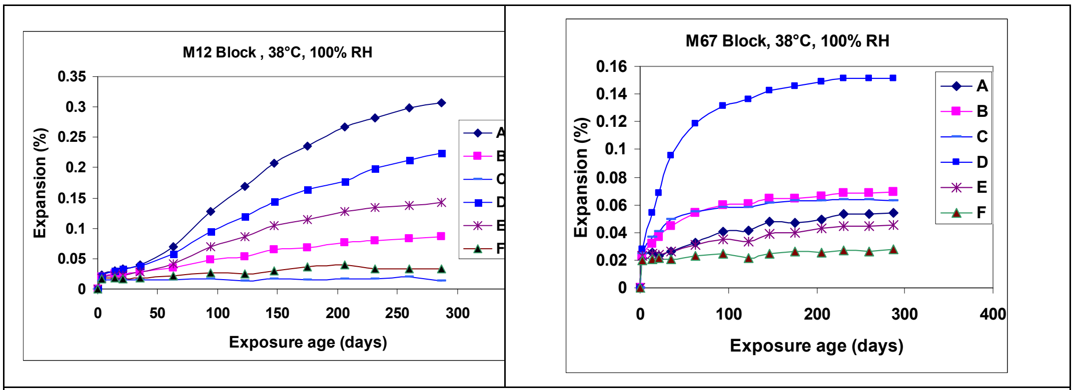

Figure 11: Expansion curves for concrete blocks stored at 38 °C, 100% RH, for planks M12 (left) and M67 (right). Measurements were made transverse (A, B, D, E) and longitudinal (C , F).

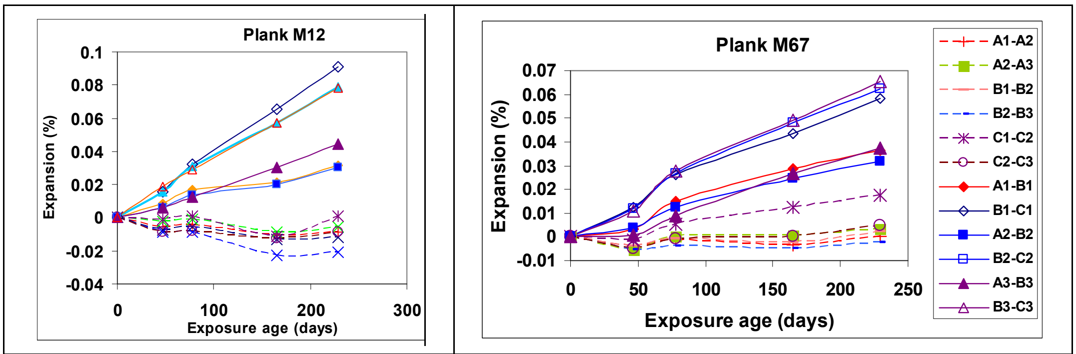

Figure 12: Expansion measurements on planks M12 (left) and M67 (right) under outdoor exposure conditions. Measurements for A1-A2, A2-A3, B1-B2, B2-B3, C1-C2, C2-C3 were longitudinal, whereas A1-B1, B1-C1, A2-B2, B2-C2, A3-B3, B3-C3 were in the transverse direction, and perpendicular to the existing parallel cracks.

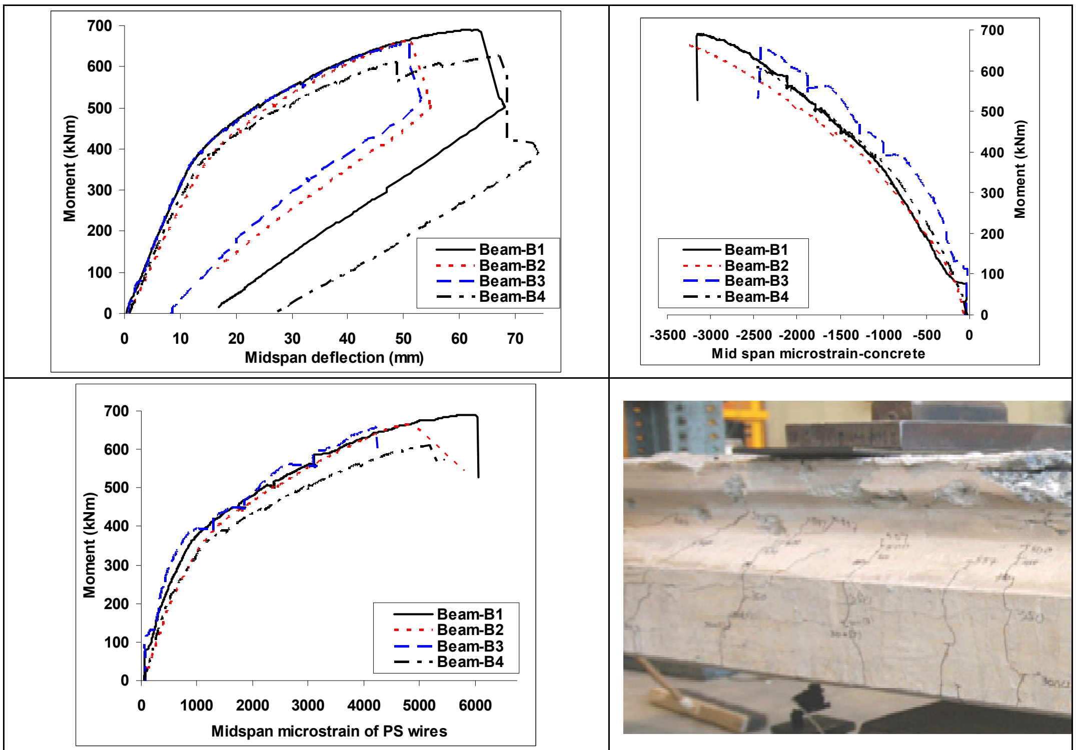

Figure 13: Moment-deflection curves for the four planks (top left); Moment versus mid-span concrete strain for all planks (top right); Moment versus mid-span steel strain for all planks (bottom left), and a plank after testing.